PROTEINS
STRUCTURE ■ FUNCTION ■ BIOINFORMATICS

STRUCTURE NOTE

Structure of the NLRP1 caspase recruitment domain suggests potential mechanisms for its association with procaspase-1

Tengchuan Jin, James Curry, Patrick Smith, Jiansheng Jiang, and T. Sam Xiao*

Structural Immunobiology Unit, Laboratory of Immunology, National Institute of Allergy and Infectious Diseases, National Institutes of Health, Bethesda, Maryland 20892-0430

ABSTRACT

The NLRP1 inflammasome responds to microbial challenges such as *Bacillus anthracis* infection and is implicated in autoimmune disease such as vitiligo. Human NLRP1 contains both an N-terminal pyrin domain (PYD) and a C-terminal caspase recruitment domain (CARD), with the latter being essential for its association with the downstream effector procaspase-1. Here we report a 2.0 Å crystal structure of the human NLRP1 CARD as a fusion with the maltose-binding protein. The structure reveals the six-helix bundle fold of the NLRP1 CARD, typical of the death domain superfamily. The charge surface of the NLRP1 CARD structure and a procaspase-1 CARD model suggests potential mechanisms for their association through electrostatic attraction.

Proteins 2013; 81:1266–1270

Key words: NLRP1; CARD; death domain fold; electrostatic attraction.

INTRODUCTION

The NOD-like receptors or nucleotide-binding domain leucine-rich repeat-containing receptors (NLRs) are a family of intracellular receptors that respond to microbial infections as well as host-derived danger signals.[1] These receptor proteins are characterized by a tripartite domain structure, with N-terminal caspase recruitment domains (CARDs) or pyrin domains (PYDs), central nucleotide-binding and oligomerization domains (NODs), and C-terminal leucine-rich repeats (LRRs). NLRP1 is one of the founding members of the NLR family, with its many variants implicated in susceptibility to vitiligo associated autoimmune and autoinflammatory diseases.[2] In addition, polymorphisms in mouse NLRP1b and rat NLRP1 were linked to susceptibility to anthrax lethal toxin-induced pyroptosis.[1,3] The human NLRP1 is unique among the NLRP proteins in that it contains both an N-terminal PYD and a C-terminal CARD, two domains of the six-helix bundle death domain fold implicated in homotypic interactions. In contrast to other NLRP

Additional Supporting Information may be found in the online version of this article.

Grant sponsor: National Cancer Institute; Grand number: Y1-CO-1020; Grant sponsor: National Institute of General Medical Sciences; Grand number: Y1-GM-1104; Grant sponsor: US Department of Energy; Grand number: DE-AC02-06CH11357; Grant sponsor: Division of Intramural Research, National Institute of Allergy and Infectious Diseases, NIH.

*Correspondence to: T. Sam Xiao, Structural Immunobiology Unit, Laboratory of Immunology, NIAID, NIH, 4 Memorial Drive, Building 4, Room 228, Bethesda, MD 20892-0430. E-mail: xiaot@niaid.nih.gov

Received 18 December 2012; Revised 26 February 2013; Accepted 2 March 2013
Published online 18 March 2013 in Wiley Online Library (wileyonlinelibrary.com).
DOI: 10.1002/prot.24287

proteins, the CARD rather than the PYD of NLRP1 appears to be essential for its recruitment of procaspase-1 and formation of a large oligomeric signaling platform known as the inflammasome,[4] as both mouse and rat NLRP1 proteins lack the N-terminal PYD. In agreement, NLRP1 directly associates with procaspase-1 through their respective CARDs in the absence of the adapter ASC.[2,5] On the other hand, the PYD of NLRP1 mediates its association with ASC, which can enhance hNLRP1 inflammasome activation.[5]

The CARD was first described as a domain involved in apoptotic signaling through homotypic associations.[6] Structural studies of the CARDs from vertebrate proteins[7,8] revealed a six-helix bundle fold similar to other members of the death domain superfamily. The only reported structure of a CARD:CARD complex at atomic resolution is that of the Apaf-1 CARD and procaspase-9 CARD, which is critically important for the assembly of the Apaf-1 apoptosome.[7] This structure illustrates electrostatic charge complementarity between the acidic α2-α3 helices of the Apaf-1 CARD and the basic α1 and α4 helices of the procaspase-9 CARD. In addition to electrostatic interactions, hydrogen bonds and van der Waals interactions also play important roles in mediating this CARD complex formation.[7] Structural studies of the IPS-1 CARD also suggested that electrostatic attractions may play a role in mediating the IPS-1 CARD and RIG-I CARD association.[8]

To examine the structure of the NLRP1 CARD and the potential mechanism of its association with the procaspase-1 CARD during inflammasome assembly, we determined the crystal structure of the NLRP1 CARD using a maltose-binding protein (MBP) fusion strategy. The structure reveals a six-helix bundle fold with prominent charged surface patches. Comparison with a procaspase-1 CARD model and the Apaf-1/procaspase-9 CARD complex suggests that electrostatic attractions may play a role in mediating the association of the NLRP1 and procaspase-1 CARDs.

Table I
X-Ray Diffraction Data Collection and Structural Refinement Statistics

Data collection	
Spacegroup	$C2_1$
Unit cell (a, b, c) (Å)	187.0, 108.8, 121.3
(α,β,γ) (°)	90, 121, 90
Wavelength (Å)	0.97
Resolution (Å)	50–2.00 (2.03–2.00)
No. of reflections (total/unique)	583,986/139,624
Redundancy	4.2 (4.0)
Completeness (%)	99.5 (99.6)
$I/\sigma(I)$	9.4 (2.7)
R_{merge} (%)	14.9 (77.5)
R_{pim} (%)	7.3 (38.7)
Refinement	
Resolution (Å)	50-2.00
Number of protein atoms/*B*-factor (Å^2)	10,786/31.4
Number of hetero-atoms/*B*-factor (Å^2)	1628/39.8
Rmsd bond lengths (Å)	0.007
Rmsd bond angles (°)	1.055
Rwork (%)	17.0
Rfree (%)	20.8
Ramachandran plot favored/disallowed	98.0/0.0
PDB code	4IFP

Numbers in parenthesis represent the highest resolution shell.
The quality of the structure was analyzed by the Molprobity server.

MATERIALS AND METHODS

Protein expression and purification

The human NLRP1 CARD (NCBI accession #NP_127497, residues 1379–1462) was cloned into a pET30a-derived vector with a non-cleavable N-terminal MBP tag and a C-terminal hexa-Histidine tag. The MBP tag harbors mutations (D82A/K83A/E172A/N173A/K239A) designed to enhance its crystallization propensity. Transformed BL21 (DE3) Codon Plus RIPL cells (Stratagene, Santa Clara, CA) were grown at 37°C and induced with 0.3 m*M* IPTG at 18°C for 4 h. The cells were lysed by sonication in buffer A (20 m*M* Tris-HCl, pH 8.0, 100 m*M* NaCl) plus 5 m*M* imidazole, DNase (Biomatik, Wilmington, DE) and protease inhibitors (Roche Applied Science, Indianapolis, IN). Soluble protein was purified from the cell lysate by Hisprep IMAC column (GE Healthcare Bio-Sciences, Piscataway, NJ). The IMAC eluted MBP-CARD protein was further purified using a XK26/60 Superdex 200 size-exclusion column (GE Healthcare Bio-Sciences, Piscataway, NJ) in buffer A supplemented with 5 m*M* maltose (Research Products International Corp, Mount Prospect, IL).

Crystallization

Purified MBP-CARD protein was concentrated using Amicon centrifugal concentrators (Millipore, Billerica, MA) to 50 mg mL^{-1} before setting up hanging drops for vapor diffusion crystallization using the Mosquito crystallization robot (TTP Labtech, United Kingdom). Multiple crystallization conditions were readily indentified using ammonium sulfate, potassium citrate, or sodium malonate as the primary precipitant. X-ray diffraction to high resolution was obtained from crystals grown with a well solution containing 1.4*M* sodium malonate and 0.1*M* HEPES-Na, pH 7.4. 20% sucrose (w/v) was added to the reservoir solution as the cryoprotectant to flash-cool the crystals in liquid nitrogen for X-ray diffraction data collection.

X-ray diffraction, structure determination, and refinement

X-ray diffraction data were collected at the GM/CA-CAT of the Advanced Photon Source, Argonne National Laboratory. Data were processed with the HKL2000 program suite[9] (Table I). The structure was determined by

molecular replacement with Phaser[10] from the CCP4 program suite.[11] A structure of the MBP from the protein data bank (PDB) (3VD8) was used as the search model. Electron density maps calculated with phases from the MBP search model clearly showed excellent densities for the NLRP1 CARD. While the structural determination was in progress, a 3.1 Å resolution crystal structure of the NLRP1 CARD was deposited and released at the PDB (3KAT), which aided our model building efforts. Model building was carried out with Coot[12] and refined with Phenix.refine.[13] The final structure contains 458 residues, of which residues L372 to K455 correspond to residues L1379 to K1462 of the NLRP1 receptor (NP_127497). A strong positive density at the carbohydrate-binding site of MBP was interpreted as a maltose. Validation of the structure by the Molprobity server[14] showed that 98.0% of all protein residues were in the favored regions of the Ramachandran plot with no outliers. Electrostatic surfaces were calculated with program Delphi (v4)[15] and displayed with Pymol (Delano Scientific LLC, San Carlos, CA).

Modeling of the caspase-1 CARD structure

A model of the human procaspase-1 CARD was produced with the I-TASSER server (http://zhanglab.ccmb.med.umich.edu/I-TASSER/),[16] using the structure of ICEBERG (1DGN) as a template, which has a 54% sequence identity with the procaspase-1 CARD. The model from the I-TASSER server has 94% of residues in the most favored region of the Ramachandran plot according to evaluation by the Molprobity server (http://molprobity.biochem.duke.edu/).[14]

RESULTS AND DISCUSSION

The NLRP1 CARD adopts a six-helix bundle fold

Our initial efforts in crystallizing the human NLRP1 CARD were unsuccessful, as the overexpressed CARD had low solubility. We employed the MBP as a fusion tag with the NLRP1 CARD and succeeded in purifying soluble, monomeric fusion proteins. The MBP tag is not only a common expression/purification tag for recombinant proteins, but it is also amongst the most successful crystallization chaperones that facilitate crystallization of challenging protein targets, including the IPS-1 CARD.[8] Our MBP-CARD fusion protein was readily crystallized and the structure was determined to 2.0 Å resolution using a structure of the MBP (3VD8) as a molecular replacement search model [Fig. 1(A) and Table I]. The interface between MBP and NLRP1 CARD is hydrophilic, with three direct hydrogen bonds and three water-mediated hydrogen bonds between the MBP and the α1 and α4 helices of the NLRP1 CARD [Fig. 1(B)]. The structure of the NLRP1 CARD is unlikely distorted by the MBP fusion tag, as evidenced by the excellent agreement between our structure and a deposited NLRP1 CARD structure 3KAT (rmsd 0.712 Å) [Fig. 1(C)]. The higher resolution and more complete diffraction data reported here likely contributed to the improved quality of our structure (Supporting Information Table SI). Representative electron density maps for the two NLRP1 CARD structures are shown in the Supporting Information Figure 1(A,B).

The NLRP1 CARD contains six anti-parallel α helices folded in a greek key arrangement, similar to other members of the death domain fold [Fig. 1(D)]. Superposition of its structure with other known CARD structures reveal a general agreement on the location of the six helices, with variations on the length and orientation of each helix [Fig. 1(D,E)]. The α6 helix of the NLRP1 CARD is involved in a crystal lattice contact, with residue W1460 at this helix in contact with its symmetry mate [Supporting Information Fig. 1(C)]. Interestingly, this same lattice contact is also present for the other NLRP1 CARD structure (3KAT) [Supporting Information Fig. 1(D)]. The physiological significance of this interface is currently unclear. Consistent with previous observations,[17] most of the conserved residues among the CARDs are hydrophobic residues involved in the packing of the hydrophobic core [Fig. 1(E)]. Structural homology search using the Dali server[18] demonstrated high structural similarity between the NLRP1 CARD and those from Apaf-1, NOD1, procaspase-9 and ICEBERG (Supporting Information Table SII).

The NLRP1 CARD exhibits prominent charged surface patches

To investigate the molecular interaction between the CARDs of NLRP1 and caspase-1, we first produced a homology model of the procaspase-1 CARD based on an NMR structure of the ICEBERG that has 54% sequence identity with the procaspse-1 CARD. Analysis of the electrostatic charge surfaces of the NLRP1 and procaspase-1 CARDs revealed that both domains contain prominent charged surface patches, with a dominant positively charged patch near their α1 and α4 helices, and a dominant negatively charged patch at their α2-α3 helices [Fig. 2(A,B)]. This is strikingly similar to the surface of the Apaf-1 and procaspase-9 CARDs [Fig. 2(C,D)]. In the Apaf-1:procaspase-9 complex, the acidic α2-α3 helices of Apaf-1 CARD [Fig. 2(C) right panel] are in contact with the basic α1 and α4 helices of the procaspase-9 CARD [Fig. 2(D) left panel]. Even though the basic α1 and α4 helices of the Apaf-1 CARD and the acidic α2-α3 helices of the procaspase-9 also have apparent charge complementarity, mutations at these regions did not diminish the Apaf-1:procaspase-9 association.[7] The Apaf-1:procaspase-9 complex structure illustrates a mechanism of

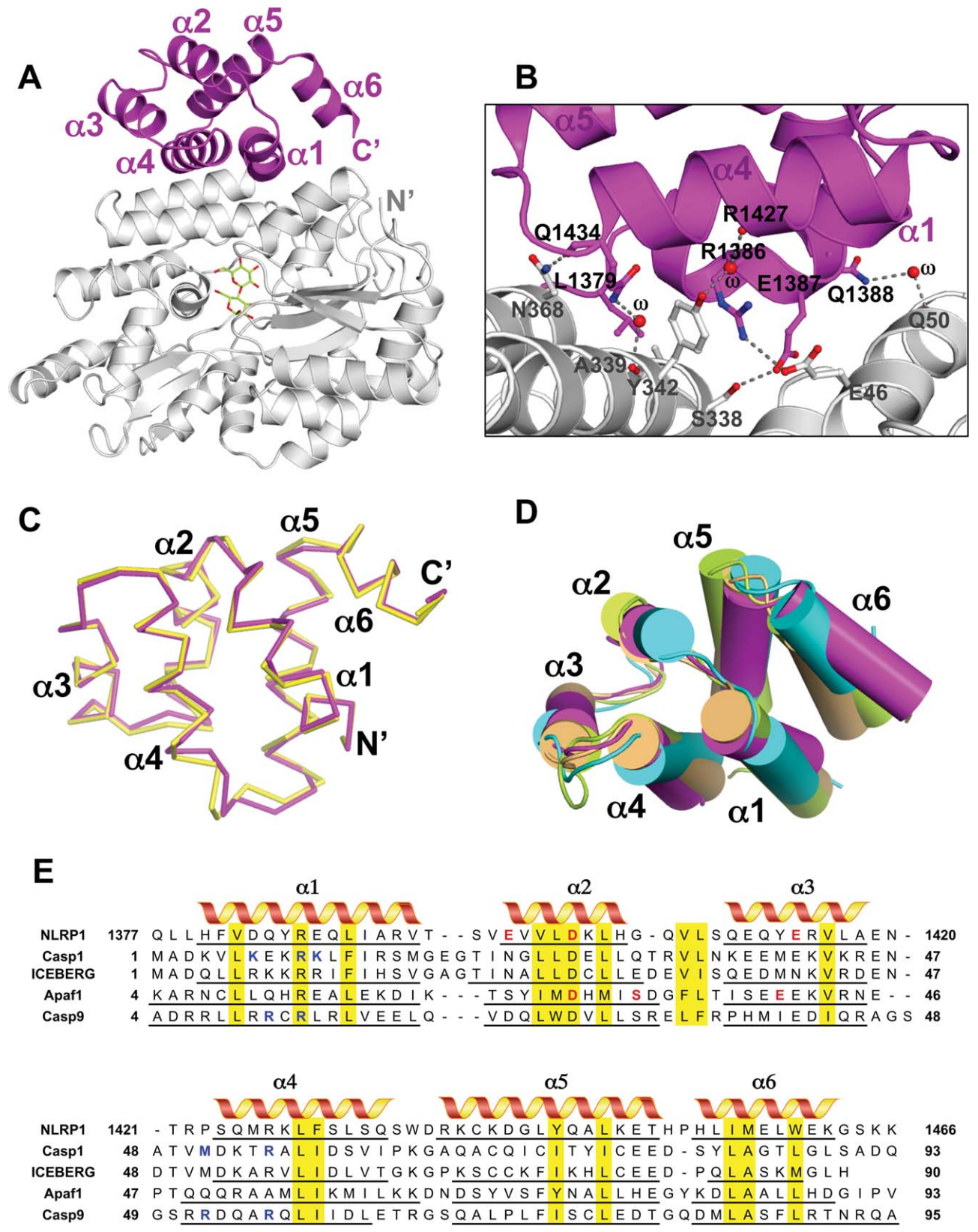

Figure 1

The NLRP1 CARD adopts a six-helix bundle fold. **A**. The MBP-NLRP1-CARD structure is shown as ribbons with the MBP colored gray and the CARD colored magenta. The six α helices of the CARD are labeled. The bound maltose at the MBP is shown as sticks. **B**. The MBP (gray) and NLRP1-CARD (magenta) associate through hydrophilic interface in the crystal. Hydrogen bonds are shown as gray dotted lines. **C**. Superposition of the MBP-NLRP1-CARD (4IFP, magenta) and NLRP1-CARD (3KAT, yellow) structures. **D**. Superposition of the CARD structures from NLRP1 (magenta), Apaf-1 (orange), procaspase-9 (green), and ICEBERG (cyan) with each helix represented as a cylinder. The view is rotated ~90° along the horizontal axis from that in C. **E**. Sequence alignment of the CARDs from NLRP1, procaspase-1, ICEBERG, Apaf-1 and procaspase-9. The six α helices of the known CARD structures are underlined and marked above the sequences. The conserved residues are shaded in yellow. The basic and acidic residues at the procaspase-9:Apaf-1 and procaspase-1:NLRP1 interface [Fig. 2(E)] are colored blue and red, respectively.

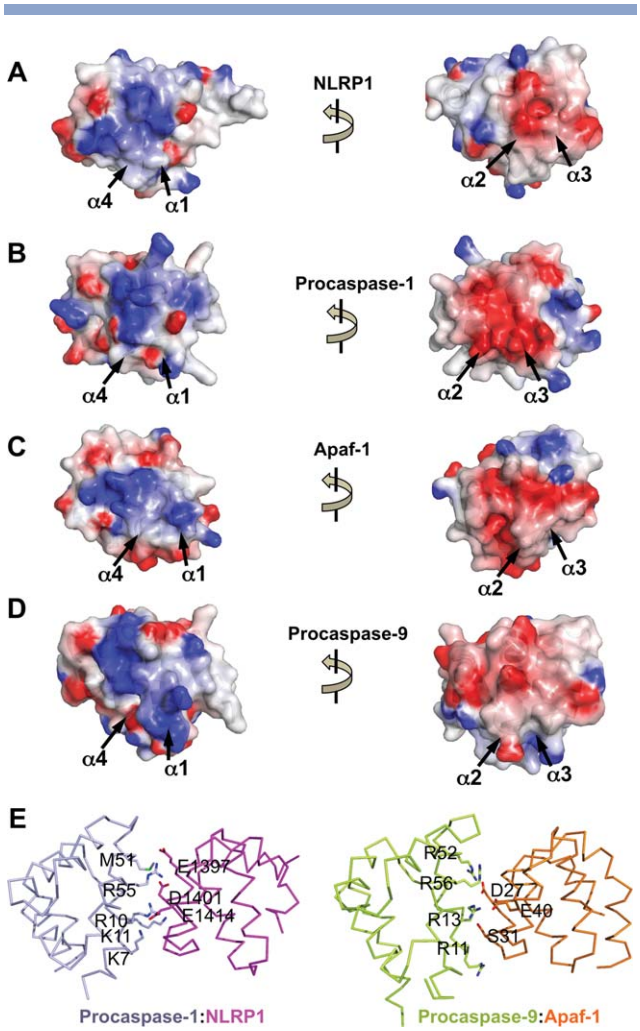

Figure 2

Electrostatic charge surface of the CARD structures. The electrostatic charge surfaces of the CARD structures from NLRP1, procaspase-1 (homology model), Apaf-1, and procaspase-9 are displayed on a scale of −5 kT/e (red) to 5 kT/e (blue) in **A–D**. The α1 and α4 helices face the viewer in the left panels, whereas the α2–3 helices face the viewer in the right panels. **E**. A model of the procaspase-1:NLRP1 CARD complex is shown on the left with the charged interface residues displayed as sticks. The procaspase-9:Apaf-1 CARD complex structure is shown on the right for comparison. [Color figure can be viewed in the online issue, which is available at wileyonlinelibrary.com.]

association mediated by a combination of hydrogen bonds, van der Waals interactions, as well as salt bridges. By analogy to the Apaf-1:procaspase-9 complex structure, it is possible that the NLRP1 CARD may associate with the procaspase-1 CARD through complementary charge surface. A possible model of such a complex is represented in Figure 2(E) (left panel), with the acidic α2-α3 helices of the NLRP1 CARD binding to the basic α1 and α4 helices of the procaspase-1 CARD, similar to the Apaf-1:procaspase-9 complex [Fig. 2(E) right panel]. Further experimental evidence is required to validate the details of the CARD:CARD complex, or whether other modes of interaction besides the charge complementarity also play a role in this CARD:CARD association.

REFERENCES

1. Davis BK, Wen H, Ting JPY. The inflammasome NLRs in immunity, inflammation, and associated diseases. Annu Rev Immunol 2011;29:707–735.
2. Jin Y, Mailloux CM, Gowan K, Riccardi SL, LaBerge G, Bennett DC, Fain PR, Spritz RA. NALP1 in vitiligo-associated multiple autoimmune disease. N Engl J Med 2007;356:1216–1225.
3. Boyden ED, Dietrich WF. Nalp1b controls mouse macrophage susceptibility to anthrax lethal toxin. Nat Genet 2006;38:240–244.
4. Martinon F, Burns K, Tschopp J. The inflammasome: a molecular platform triggering activation of inflammatory caspases and processing of proIL-beta. Mol Cell 2002;10:417–426.
5. Faustin B, Lartigue L, Bruey J-M, Luciano F, Sergienko E, Bailly-Maitre B, Volkmann N, Hanein D, Rouiller I, Reed JC. Reconstituted NALP1 inflammasome reveals two-step mechanism of caspase-1 activation. Mol Cell 2007;25:713–724.
6. Hofmann K, Bucher P, Tschopp J. The CARD domain: a new apoptotic signaling motif. Trends Biochem Sci 1997;22:155–156.
7. Qin H, Srinivasula SM, Wu G, Fernandes-Alnemri T, Alnemri ES, Shi Y. Structural basis of procaspase-9 recruitment by the apoptotic protease-activating factor 1. Nature 1999;399:549–557.
8. Potter JA, Randall RE, Taylor GL. Crystal structure of human IPS-1/MAVS/VISA/Cardif caspase activation recruitment domain. BMC Struct Biol 2008;8:11.
9. Otwinowski Z, Minor W. Processing of X-ray diffraction data. Meth Enzymol 1997;276:307–326.
10. McCoy AJ, Grosse-Kunstleve RW, Adams PD, Winn MD, Storoni LC, Read RJ. Phaser crystallographic software. J Appl Crystallogr 2007;40 (Part 4):658–674.
11. Potterton E, Briggs P, Turkenburg M, Dodson E. A graphical user interface to the CCP4 program suite. Acta Crystallogr D Biol Crystallogr 2003;59:1131–1137.
12. Emsley P, Cowtan K. Coot: model-building tools for molecular graphics. Acta Crystallogr D Biol Crystallogr 2004;60:2126–2132.
13. Adams PD, Afonine PV, Bunkóczi G, Chen VB, Davis IW, Echols N, Headd JJ, Hung L-W, Kapral GJ, Grosse-Kunstleve RW, McCoy AJ, Moriarty NW, Oeffner R, Read RJ, Richardson DC, Richardson JS, Terwilliger TC, Zwart PH. PHENIX: a comprehensive Python-based system for macromolecular structure solution. Acta Crystallogr D Biol Crystallogr 2010;66:213–221.
14. Chen VB, Arendall WB, Headd JJ, Keedy DA, Immormino RM, Kapral GJ, Murray LW, Richardson JS, Richardson DC. MolProbity: all-atom structure validation for macromolecular crystallography. Acta Crystallogr D Biol Crystallogr 2010;66:12–21.
15. Honig B, Nicholls A. Classical electrostatics in biology and chemistry. Science 1995;268:1144–1149.
16. Roy A, Kucukural A, Zhang Y. I-TASSER: a unified platform for automated protein structure and function prediction. Nat Protoc 2010;5:725–738.
17. Park HH, Lo Y-C, Lin S-C, Wang L, Yang JK, Wu H. The death domain superfamily in intracellular signaling of apoptosis and inflammation. Annu Rev Immunol 2007;25:561–586.
18. Holm L, Rosenstrom P. Dali server: conservation mapping in 3D. Nucleic Acids Res 2010;38:W545–W549.